



**Students'  
Space Association**  
WARSAW UNIVERSITY OF TECHNOLOGY



Coordinator: Szymon Życiński  
Date: 21/02/2024  
Number of pages: 11

Author(s): Bartosz Dabrowski

# Development of T800 sounding rocket solid motor

Lessons learned from the fight with internal ballistics



---

# Contents

<b>1</b>	<b>Introduction</b>	<b>1</b>
<b>2</b>	<b>Mission requirements</b>	<b>2</b>
<b>3</b>	<b>Internal ballistics simulation</b>	<b>2</b>
<b>4</b>	<b>Structural design</b>	<b>7</b>
4.1	Casing . . . . .	7
4.2	Nozzle assembly . . . . .	7
4.3	Forward closure assembly . . . . .	8
<b>5</b>	<b>Real world validation</b>	<b>10</b>
<b>6</b>	<b>Summary</b>	<b>10</b>
<b>7</b>	<b>Bibliography</b>	<b>11</b>



---

## 1 Introduction

The primary objectives of the Ascension project are centered around achieving specific milestones with motor performance constraints to validate and enhance key aspects of sounding rocket technology. These objectives include rigorously testing recovery, propulsion, and launch logistics. The combination of these objectives serves as a robust platform for evaluating and refining the technology for future atmospheric research applications while proving our capability to perform such tasks in safe and professional manner.

The Ascension-3 sounding rocket is meticulously designed to meet the altitude and velocity targets set for the project while staying under M class limit. A key focus is placed on the propulsion system, where the T800 solid rocket motor incorporates many technologies to ensure optimal thrust and reliability. The motor's composition and combustion characteristics are engineered to facilitate the desired performance, providing critical insights into propulsion capabilities for future projects.

Main goals for this project was to ensure motor's structural integrity, stability, and overall simplicity as it directly correlates with mission success rate. A series of ground tests and multiple flight tests are conducted to validate the rocket's performance under real-world conditions. These tests allow for iterative refinements to the design based on empirical data, contributing to the overall success of the project.



## 2 Mission requirements

Structural design of the rocket was tied to already available 85x2.5mm fiberglass filament wound tubing for the airframe. To accommodate all the necessary electronics for a safe flight and successful recovery, the nosecone was made mostly to fit payload, not for performance. Ogive shape, featuring a 6:1 L/D ratio, was chosen.

In a nod to a previous rocket project where this motor was intended to be a part of, the fins were designed in the distinctive LERX-delta shape. Although this design excels in high Angle of Attack (AoA) scenarios, it's worth noting that such performance attributes hold less relevance in the context of sounding rocketry.

For the recovery system, we implemented a drougue-main architecture. The drougue parachute was deployed at apogee, ensuring stability during the descent. At a specified altitude Above Ground Level (AGL), the main parachute was released, facilitated by a in-house developed pyrotechnical cable cutter. This recovery setup was designed to enhance safety and precision throughout the entire flight and landing sequence.

After completing initial design calculated vehicle parameters were as follows [1]:

Table 1: Asension-3 technical specification

Length	2150	mm
Diameter	85	mm
Mass	12	kg
Motor impulse	Under 5120 <i>Ns</i> to stay under L3 limit [2]	

## 3 Internal ballistics simulation

Solid motor is a complex system that combines many physical phenomena and thus we need a simplified mathematical model to reasonably predict and simulate propellant behaviour at different conditions. During design I assumed an ideal rocket motor[1].

For propellant Saint's Robert law was used given by the equation:

$$r = a * P^n$$

where  $r$  is regression rate,  $P$  is pressure and  $a, n$  are propellant specific constants.

Another equation which was used is derived from adiabatic flow[1] and has a form of differential equation which describes pressure change in the combustion chamber.

$$\frac{v_0}{R * T_0} * \frac{dP_0}{dt} = A_b * a * P_0^n * \rho_p - P_0 * A_t * \sqrt{\frac{k}{R * T_0}} * \left(\frac{2}{k+1}\right)^{\frac{k+1}{2*(k-1)}}$$



---

Symbols used in the equation:

1.  $v_0$  - free volume within the chamber
2.  $R$  - gas constant
3.  $T_0$  - chamber temperature
4.  $P_0$  - chamber pressure
5.  $t$  - time
6.  $A_b$  - burning area
7.  $a$  - propellant pressure coefficient
8.  $n$  - propellant pressure exponent
9.  $\rho_p$  - propellant density
10.  $A_t$  - nozzle throat area
11.  $k$  - propellant specific heat ratio

This provides an easy way to iteratively simulate pressure and mass flow in our rocket motor. When we have combustion chamber pressure, we can calculate motor thrust and integrate total impulse.

All above equations were incorporated into motor simulation software written in C programming language. This provided an ample way to simulate and optimize motor parameters.

Propellant chosen for the project was potassium nitrate-sorbitol mix due to its relative availability and low cost. Parameters of such propellant are as follows[1]:

Initial grain dimensions were calculated using neutral bates equation[3]

$$L = 0.5 * (3 * D_o + D_i)$$

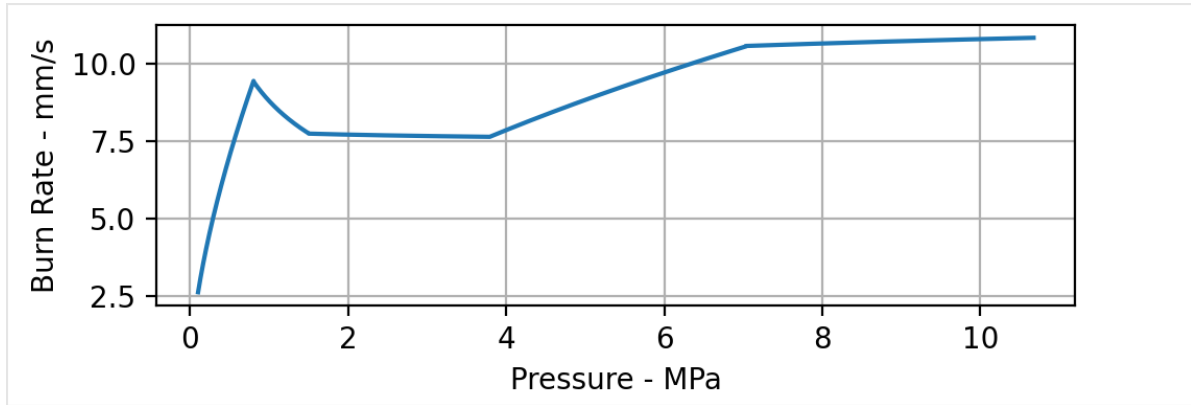
where  $L$  is ideal length,  $D_o$  and  $D_i$  are outer and inner grain diameters.

Propellant used in this project is KNSB propellant with ratios proposed by Nakka[1] with slight modification which was use of bimodal particle size to improve pourability. Pressure coefficients and pressure exponents used are were also given by Nakka. Note that KNSB changes its behaviour depending on pressure so 6 pressure ranges were used.



Table 2: KNSB propellant specification

KNO <sub>3</sub> -C <sub>6</sub> H <sub>14</sub> O <sub>6</sub> ratio	65:35	
Density	1841	$\frac{kg}{m^3}$
Burn rate coefficient	7.852	$\frac{mm}{s * Pa^n}$
Burn rate exponent	-0.013	
Specific heat ratio k	1.136	
Combustion temperature	1520	K
Exhaust molar mass	39.9	$\frac{g}{mol}$
Characteristic velocity	885	$\frac{m}{s}$



KNSB burnrate

According to the plot this particular propellant has a plateau between 2 and 4 MPa and that is the range I decided to stay in as going much higher does not necessarily result in better performance given need for thicker casings.

Nozzle optimal expansion ratio was calculated using equation:

$$\frac{A_t}{A_e} = \frac{k+1}{2}^{\frac{1}{k-1}} * \frac{P_e^{\frac{1}{k}}}{P_0} * \sqrt{\frac{k+1}{k-1} * \left(1 - \frac{P_e^{\frac{k-1}{k}}}{P_0}\right)}$$

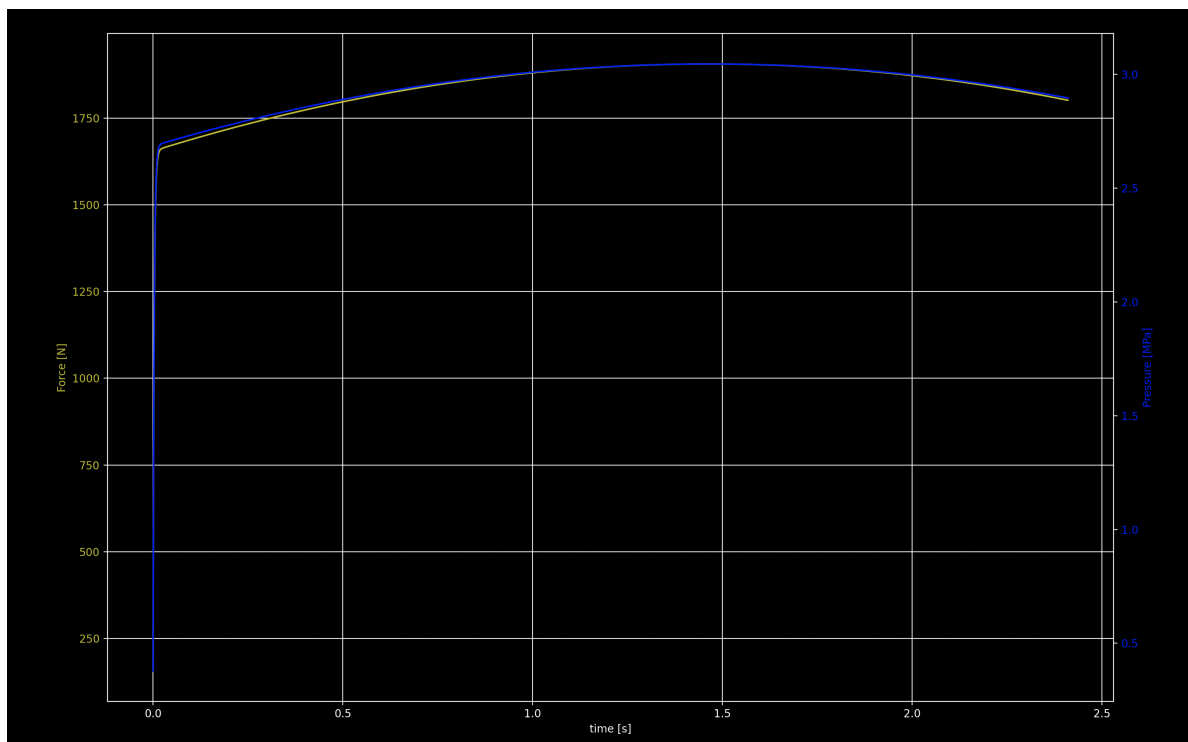
1.  $A_t$  - throat diameter
2.  $A_e$  - exit diameter
3.  $P_e$  - exit pressure



Calculations for maximum chamber pressure resulted in optimal expansion ratio of 5.37 but due to manufacturing limits ratio of 4 was used instead. This change resulted in 0.8% change in specific impulse. Calculated nozzle exit pressure was 1.47bar  
Additional length-size optimization lead to final motor specification:

Table 3: T800 parameters

Number of grains	6	
Grain outer diameter	68	mm
Grain inner diameter	29	mm
Grain length	125	mm
Propellant mass	3.82	kg
Throat diameter	24	mm
Expansion ratio	4	
Nozzle exit pressure	1.47	bar
Impulse	4431	Ns
Peak pressure	3.05	MPa
Average pressure	2.5	MPa
Peak mass flux	2628.24	$\frac{kg}{m^2*s}$
ISP	118	s

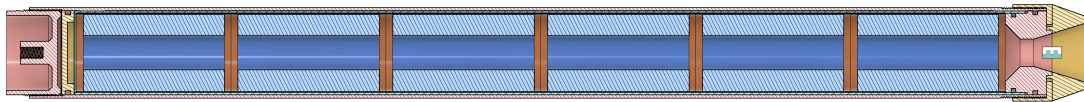


T800 simulated operation



## 4 Structural design

Main goals of T800 motor development was to find best processes regarding motor manufacturing and put our hardware design rules to the test while staying under 5120Ns of impulse due to legal reasons. Design phase started as early as January 2023 and ended in December same year.



T800 motor cross section

### 4.1 Casing

The casing was machined from 80x3 PA38 tubing with threaded closures, providing sturdy foundation for our motor development. In our structural simulations, we ensured a safety factor of 2 for a simulated Maximum Expected Operating Pressure (MEOP) of 6 MPa, offering us ample room for experimenting with propellant geometry and throat sizes.

As for stress calculations I used excel custom spreadsheet made for pressure vessel calculation. Basic assumptions are that maximum allowable stress should not exceed material yield stress divided by safety factor of 2. Using hoop stress formula

$$\sigma = \frac{p * a}{t}$$

where  $p$  is internal pressure,  $a$  is external diameter and  $t$  is wall thickness. Axial load on casing could be neglected as it's 2 times smaller than hoop stress. PA38 specification used was provided by a supplier.

Opting for cost-effectiveness, we selected PFCP21 phenolic-paper composite tubing for the thermal insulation of the casing. This choice not only proved economical but also delivered state of the art thermal protection.

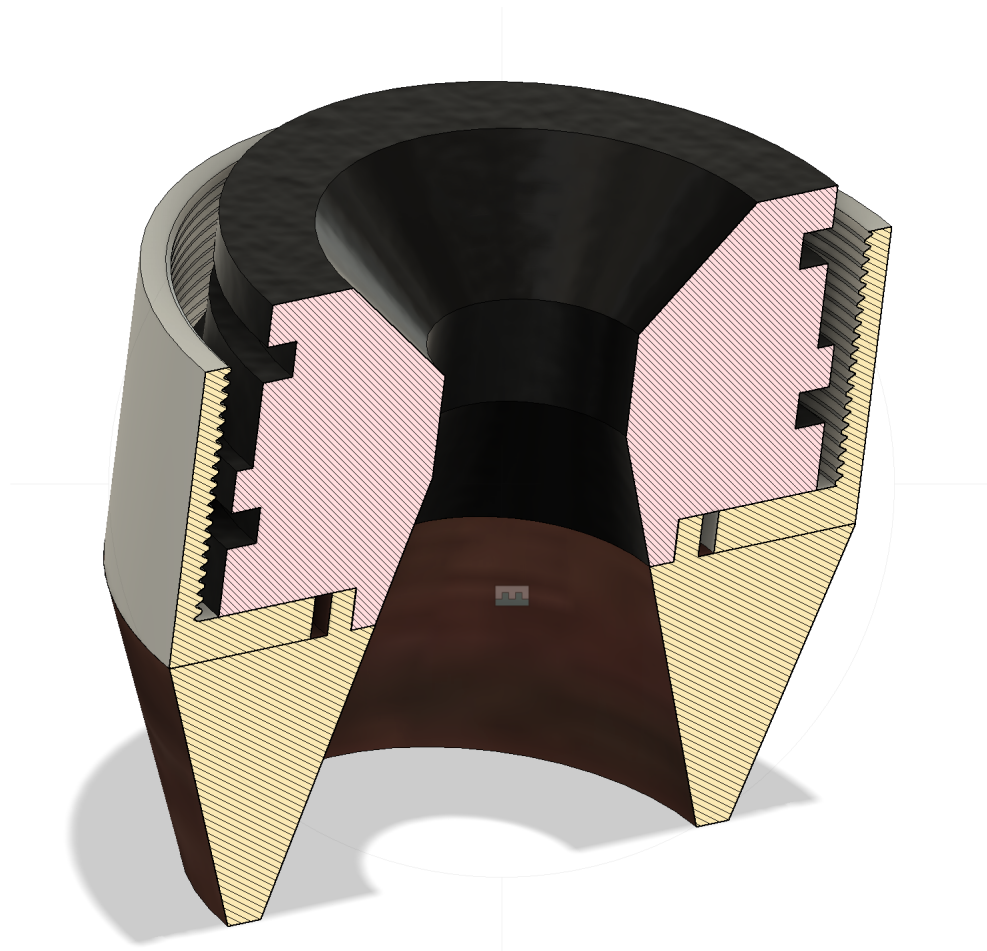
### 4.2 Nozzle assembly

Nozzle was designed in 3 parts, external threaded closure made from same PA38 aluminium with M76x2 thread, graphite nozzle insert that's meant to withstand enormous heat load during motor operation and single use linen-phenolic nozzle extension which



provides optimal expansion ratio while also reducing aerodynamic drag caused by abrupt geometry changes.

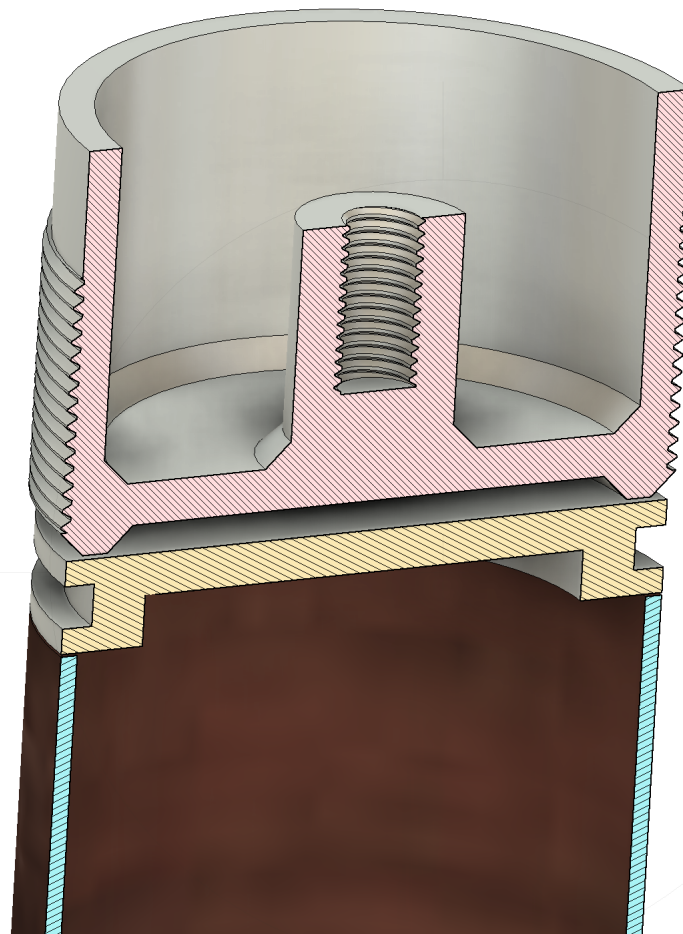
Nozzle inlet and exit shape was conical due to high solid loading of the propellant exhaust which in bell shaped nozzles may result in faster material erosion. This phenomenon is caused by greater centripetal accelerations in these shapes.



T800 nozzle assembly

### 4.3 Forward closure assembly

After conducting numerous static firings, we made a strategic decision to leave the top of the liner unsealed. This design choice facilitated pressure equalization, preventing liner cracking. This approach, with the top chosen for its higher static pressure, lower mass flux, and longer path to the aft seals, ultimately maximized the overall safety of the motor.



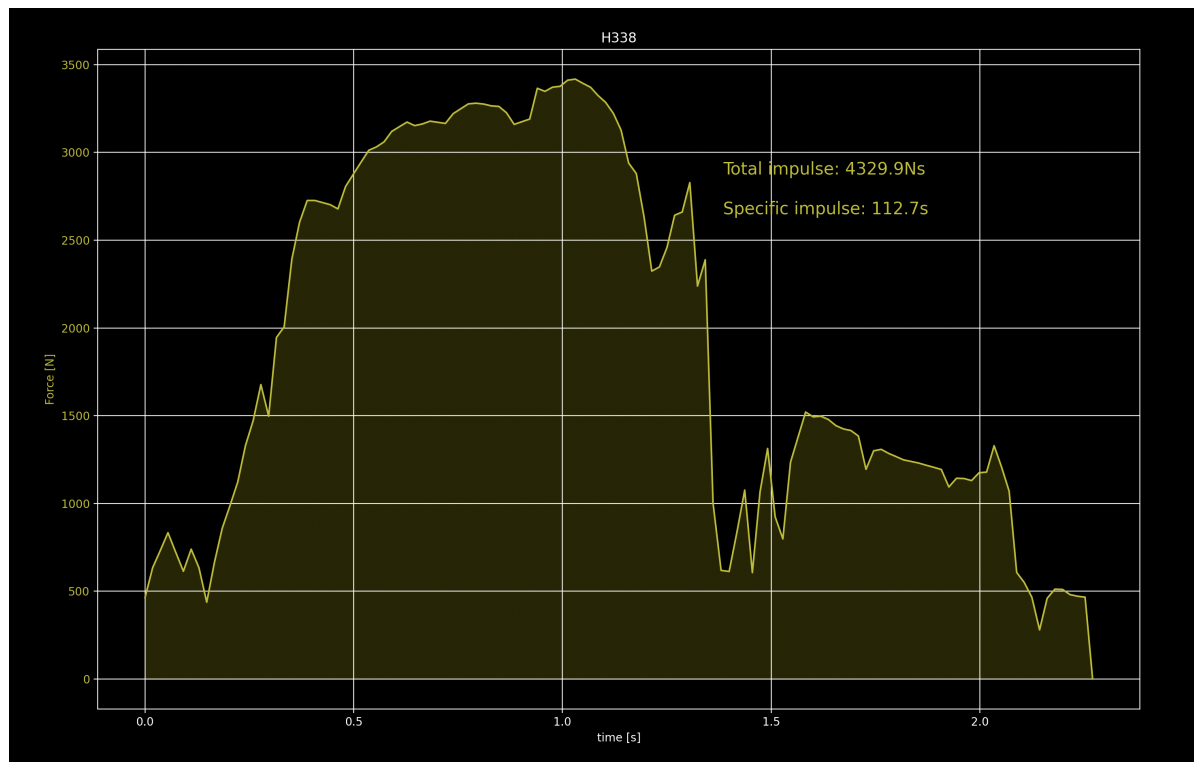
T800 forward closure assembly

While forward closure consisted only of one O-ring seal, aft closure was designed to use primary seal between liner and graphite and backup graphite-casing seal. Such a design was chosen due to higher heat and mass fluxes on aft side of the motor, resulting in faster seal deterioration.



## 5 Real world validation

It may be a surprise for some people but simulations don't always exactly match real world results. This was the case during T800 static test. We encountered a lot of problems with ignition resulting in lower ISP. During the test, two aft grains unexpectedly debonded from their respective casting tubes, causing a significant increase in burn rate. While the casing withstood the pressure, nozzle sustained major damage, resulting in a time-thrust graph that deviated from our simulated expectations.



T800 thrust curve

## 6 Summary

Embarking on the development of the T800 sounding rocket motor proved to be a challenging yet profoundly rewarding journey. The experience enriched our understanding of the intricate workings within solid rocket motors, offering invaluable insights that surpassed our initial expectations. It served as a masterclass in iteratively solving complex engineering problems, refining our approach at each turn.

While the motor's performance may not have reached stellar heights, the wealth of knowledge gained positions us confidently for the final flight. The T800 project has not



---

only advanced our technical expertise but has also instilled a deep sense of readiness and anticipation for the culmination of this remarkable endeavor.

## 7 Bibliography

### References

- [1] Richard Nakka *Experimental Rocketry Web Site*
- [2] National Association of Rocketry (2012) *High Power Rocket Safety Code*
- [3] John S. DeMar (2006) *Basic Experimental Solid Propellant Motors*